Laterally Resolved Microwave Surface-Resistance Measurement of High-T_C Superconductor Samples by Cavity Substitution Technique

Mukul Misra, N. D. Kataria, and G. P. Srivastava, *Senior Member, IEEE*

***Abstract*—Microwave surface impedance measurement of a high-temperature superconductor (HTS) is a sensitive probe to test its quality, particularly if a microwave device is to be fabricated. Most microwave characterization employs resonance techniques in which the components of the surface impedance are extracted from the measured Q value and the shift in the resonance frequency. In this paper, we present a modification of the widely used complete end-plate substitution technique to measure the surface resistance of samples having dimensions smaller than the dimension of the end plate at 20 GHz, as well as to facilitate the laterally resolved surface resistance measurement of large-area HTS samples. From the knowledge of the electromagnetic-field configuration in a TE_{011}-mode cylindrical cavity, the loss contribution from the HTS sample is analyzed theoretically and measured experimentally in the temperature range of 20–100 K. The design of the cavity is discussed to optimize the sensitivity of the measurement by the placement of the sample and to maximize the difference in the measured Q value.**

***Index Terms*—High-temperature superconductor, microwave cavity resonator, surface resistance.**

I. INTRODUCTION

CHARACTERIZATION of high-temperature superconductor (HTS) materials at microwave frequencies is of considerable interest because it not only gives information that is useful in the design of HTS-based passive devices, but it also gives useful information to understand the conduction and energy dissipation mechanisms. The interaction of the microwave fields and superconductors is experimentally determined by the measurement of surface impedance Z_s $(=R_s + iX_s)$. The real part of Z_s, R_s, the surface resistance, characterizes the dissipated microwave power and yields information on the transport mechanism in superconductors. Technologically, R_s determines the quality of the microwave devices and circuits that can be fabricated using HTS material. The imaginary part, surface reactance X_s, is directly proportional to the magnetic penetration depth λ. The temperature dependence of λ, $\lambda(T)$ provides a direct insight into the pairing mechanism of the superconducting state, when extrinsic effects are eliminated.

Manuscript received February 23, 1999. The work of M. Misra was supported by the Council of Scientific and Industrial Research under a research fellowship award.

M. Misra and N. D. Kataria are with the Superconductivity Division, National Physical Laboratory, New Delhi 110 012, India.

G. P. Srivastava is with the Department of Electronic Sciences, University of Delhi, New Delhi 110 021, India.

Publisher Item Identifier S 0018-9480(00)03768-6.

Microwave measurements have been used since the early stage of superconductivity. Pippard [1] reported the study of penetration depth in classical superconductors, such as Pb, using a microwave cavity resonator. Since then, various configurations with improved precision, sensitivity, and reliability have been employed to study the surface impedance of superconducting materials [2]. Most of the techniques used for R_s measurement are resonant methods [3]–[7] where R_s is calculated from the measured quality factor of a resonating structure. In the cylindrical-cavity end-plate substitution technique, the surface resistance of the sample is extracted from the measured Q value of the TE_{011} mode cavity without and with the sample substituting one of the end plates. The size of the sample that can completely substitute the end plate decides the frequency of operation of such a cavity. For the measurement of the samples of HTS thin films usually deposited on 10 mm $\times$ 10 mm substrates, the cavities are designed at frequencies greater than $\sim$40 GHz. In [8] and [9], we reported measurement of the surface resistance of HTS samples of dimensions smaller than the cavity end plate, by the partial end-plate substitution technique at 10 and 20 GHz. In this method, the sample of radius $d (d < a)$ substitutes a circularly symmetric opening at the center of the end plate of the cavity. The expression for extracting R_s from the Q measurement is modified by separately calculating the losses due to the sample exposed to the microwaves. A similar method of measurement is also employed by Silva *et al.* [10] to measure the surface resistance of Bi : 221 2 thin films of different areas by shadowing the sample with a thin metal mask. Moreover, our method can also be employed for the R_s mapping to deduce the lateral R_s homogeneity over large-area HTS thin films using masks with different circular openings on top of it. The laterally resolved R_s measurement provides very important information for control of lateral homogeneity of thin film deposition process [11].

In this paper, we report laterally resolved surface resistance measurement of YBCO bulk and thin films by the cavity resonator technique at 20 GHz. An expression to extract the R_s value from the measured unloaded Q value of the cavity-containing sample, having dimension smaller than its end plate, has been obtained from TE_{011}-mode electromagnetic-field configuration inside a cavity using proper boundary conditions. Finally, the expression is used to analyze theoretically the dependence of sensitivity of the measurement on the size of the sample as well as on the aspect ratio $(2a/L)$ of the cavity, where a and L are, respectively, the radius and length of the cylindrical cavity.

II. Cavity Resonator Technique

Cylindrical cavity resonators have been extensively used for measuring the microwave properties of an HTS. Two different measurement schemes based on different principles are employed for this purpose: 1) perturbing the electromagnetic field by placing the sample at the position of the maximum electric or magnetic field inside the cavity, i.e., the cavity perturbation technique [7] and 2) substituting the end wall of the cavity by the sample, i.e., the complete end-plate substitution technique [6]. In both of the techniques, the surface resistance of the sample is estimated from the change in the unloaded Q value of the cavity with and without the sample. The unloaded Q value Q_o is the figure-of-merit for assessing the performance or quality of a resonator, defined as

$$Q_0 = 2\pi \frac{\text{maximum energy stored in the cavity}}{\text{average energy dissipated per cycle}} = 2\pi f_o \frac{W_t}{P_l}$$

where f_0 is the resonant frequency, W_t is the total energy stored, and P_l is the average power loss. In the case of a hollow cavity resonator, power dissipates only due to conduction loss that arises as a result of finite conductivity of the cavity walls. The dielectric and radiation loss are negligible compared to the conductive loss, therefore, Q_o can be expressed as

$$\frac{1}{Q_0} = \frac{1}{2\pi f_0} \frac{R_s \int |\overline{J}_s|^2 \, dS}{\varepsilon_0 \int_{\text{cavity}} |\overline{E}|^2 \, dV} \tag{1}$$

where R_s is the surface resistance of the material of the walls of the cavity. ε_0 is the permittivity of the medium enclosed (free space) by the cavity walls. $\overline{J}_s$ is the surface current for perfectly conducting walls and can be deduced from the component of the magnetic field $\overline{H}$ parallel to the surface of the cavity wall by the relation

$$\overline{J}_s = \hat{n} \times \overline{H} \tag{2}$$

where $\hat{n}$ is the unit vector normal to the surface of the cavity wall. Modes of cylindrical cavity resonator of length L are designated as TE_{mnp} or TM_{mnp} with

$$(\omega/c)^2 = k_{mn}^2 + (p\pi/L)^2$$

where $k_{mn} = (2\pi/\lambda_{mn})$ is the appropriate cutoff wavelength, c is the velocity of light, and p is the number of half-wavelengths along the axis of the cavity. The modes of a circular cylindrical cavity are characterized by the radial and azimuthal dependence of the longitudinal component of field. Generally, the cylindrical cavities operating at TE_{011} mode have been extensively used to characterize the HTS materials at microwave frequencies. The cylindrical body being fabricated from a good conductor or low-temperature superconductor (LTS) [7]. The selection of the TE_{011} mode for the measurement is made due to the following reasons.

1) Accurate measurement of surface resistance requires the value of unloaded quality factor Q_0 to be as high as possible and the losses due to introduction of the specimen should be measurable. In a right cylindrical cavity, the smallest volume cavity has a TE_{0np} mode for a given Q_0 and f_0.
2) The electromagnetic-field configuration inside the cavity with the TE_{0np} mode is such that the electric field is entirely azimuthal with no radial component. As long as circular symmetry is preserved, no currents flow normal to the cylindrical axis, thus allowing replacement of the end plate without disturbing the current and electromagnetic field distribution in the cavity.
3) TE_{0np} modes are axially symmetric, which makes them suitable to use for studying the microwave properties of HTS thin films and bulk samples by a partial end-plate substitution technique.

The resonance frequency f_o of the TE_{011} mode in a cylindrical cavity resonator can be calculated from the relation

$$f_0 = \frac{c}{2\pi} \left(\alpha_1^2 + \alpha_2^2\right)^{1/2} \tag{3}$$

where $\alpha_1 = (\pi/L)$ and $\alpha_2 = (\chi'_{01}/a)$, $\chi'_{01} = 3.8317$ is the first zero of the first derivative of the Bessel function of the first kind and order zero.

III. Analysis of Cylindrical Cavity for End-Plate Substitution

The quantitative analysis of the TE_{011}-mode cylindrical cavity is well known and commonly used for measurement. However, for the special case of substituting a sample of dimension smaller than the end plate, the field equations need to be analyzed to evaluate the losses introduced by the sample. As the sample replaces the end-wall material symmetrically from its center, the introduction of the sample in the cavity will not effect the electromagnetic-field configuration or resonance frequency, which may happen due to the position of the sample when not placed symmetrically inside the cavity.

Consider a cylindrical cavity of radius a and length L whose top end plate, cylindrical sidewalls, and bottom end-plate materials have surface resistance values R_{st}, R_{ss}, and R_{sb}, respectively. The center of the bottom end plate is substituted by the sample under investigation having radius "d" with surface resistance value $R_{s\text{sample}}$, as shown in Fig. 1. The electromagnetic-field configuration of the TE_{011} mode in a cylindrical cavity is given by [12]

$$\overline{E}_\phi = i\left(\alpha_1^2 + \alpha_2^2\right)^{1/2} \alpha_2 (\mu/\varepsilon)^{1/2} J'_0(\alpha_2 \rho) \sin(\alpha_1 z) \tag{4a}$$

$$\overline{H}_z = -\alpha_2^2 J_0(\alpha_2 \rho) \sin(\alpha_1 z) \tag{4b}$$

$$\overline{H}_\rho = -\alpha_1 \alpha_2 J'_0(\alpha_2 \rho) \cos(\alpha_1 z) \tag{4c}$$

$$\overline{E}_z = 0, \quad \overline{E}_\rho = 0, \quad \overline{H}_\phi = 0 \tag{4d}$$

where $J_0(\alpha_2 \rho)$ and $J'_0(\alpha_2 \rho)$ are the Bessel functions of the first kind and order zero and the derivative of the Bessel function of the first kind and order zero, respectively.

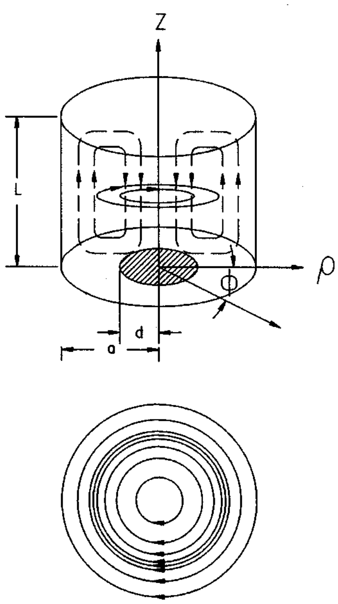

Fig. 1. TE_{011}-mode electromagnetic-field configuration and RF current distribution at the end plate of cylindrical cavity resonator.

The average energy stored W_t inside the cavity and ohmic loss P_l in the walls of the cavity are obtained using (4); applying boundary conditions yields the general expression for the unloaded quality factor Q_{os} of a TE_{011}-mode cylindrical cavity containing a sample as (see the Appendix)

$$\frac{1}{Q_{os}} = \frac{2}{Z_0}\frac{1}{a^2L}\frac{1}{(\alpha_1^2+\alpha_2^2)^{3/2}} \cdot \left[a^2\alpha_1^2R_{st} + aL\alpha_2^2R_{ss} + d^2\alpha_1^2\eta(d)R_{ssample} + d^2\alpha_1^2\left\{\frac{a^2}{d^2} - \eta(d)\right\}R_{sb}\right] \quad (5)$$

where $Z_0 = \sqrt{\mu_0/\varepsilon_0}$ is the impedance of free space and

$$\eta(d) = \left[\frac{J_1^2(\alpha_2 d)}{J_0^2(\alpha_2 a)}\left\{1 - \frac{2}{\alpha_2 d}\frac{J_0(\alpha_2 d)}{J_1(\alpha_2 d)}\right\} + \frac{J_0^2(\alpha_2 d)}{J_0^2(\alpha_2 a)}\right]. \quad (6)$$

The above equation gives the unloaded Q value Q_{os} of a cylindrical cavity, containing a sample, in terms of its dimensions and the surface resistance values of its walls. Let us consider the practical case that, except for the sample portion, all other walls of the cavity are made of copper having surface resistance R_{scu}, then $R_{st} = R_{ss} = R_{sb} = R_{scu}$. The unloaded Q value Q_{os} of the cavity containing a sample can then be written as

$$\frac{1}{Q_{os}} = \frac{2}{Z_0}\frac{1}{a^2L}\frac{1}{(\alpha_1^2+\alpha_2^2)^{3/2}} \cdot \left[\left\{2a^2\alpha_1^2 + aL\alpha_2^2 - d^2\alpha_1^2\eta(d)\right\}R_{scu} + d^2\alpha_1^2\eta(d)R_{ssample}\right] \quad (7)$$

which can be simplified as

$$\frac{1}{Q_{os}} = \left[\left\{\frac{1}{G} - \frac{1}{S(d)}\right\}R_{scu} + \frac{1}{S(d)}R_{ssample}\right] \quad (8)$$

where

$$\frac{1}{G} = \frac{2}{Z_0}\frac{1}{a^2L}\frac{1}{(\alpha_1^2+\alpha_2^2)^{3/2}}\left\{2a^2\alpha_1^2 + aL\alpha_2^2\right\} \quad (9)$$

and

$$\frac{1}{S(d)} = \frac{2}{Z_0}\frac{1}{a^2L}\frac{1}{(\alpha_1^2+\alpha_2^2)^{3/2}}\left\{d^2\alpha_1^2\eta(d)\right\}. \quad (10)$$

Here, G can be termed as the geometrical factor of the total cavity and $S(d)$ as the geometrical factor of the sample inside the cavity. The surface resistance of the sample $R_{ssample}$ can be evaluated from the measured unloaded Q value Q_{os} using (8) as

$$R_{ssample} = \left[\frac{1}{Q_{os}} - \left\{\frac{1}{G} - \frac{1}{S(d)}\right\}R_{scu}\right]S(d) \quad (11)$$

or using Q_{oc} $(=G/R_{scu})$, the measured unloaded Q value of the homogeneous copper cavity

$$R_{ssample} = \left[R_{scu} - \left\{\frac{1}{Q_{oc}} - \frac{1}{Q_{os}}\right\}S(d)\right]. \quad (12)$$

The above relation gives the measure of the surface resistance of the sample in terms of the measured unloaded Q values of all the copper cavity Q_{oc} and the cavity with a sample Q_{os}. However, for HTS thin films, Klein *et al.* [13] pointed out that the thickness of film (t) compared to the penetration depth (λ) is crucial to distinguish between the effective (measured) surface resistance $R_{ssample}$ and the characteristic (intrinsic) surface resistance R_{sc} of the film. The determination of R_{sc} requires a correction in experimentally measured $R_{ssample}$ of the thin films. Hartemann [14] used conventional transmission-line theory and a two-fluid model to obtain a relation between $R_{ssample}$ and R_{sc} and showed that for thickness of film 3λ, a film practically behaves as a bulk material.

IV. Sensitivity and Cavity Design Parameters

In this section, we shall discuss the dependence of sensitivity of the measurement on the size of the sample as well as on the aspect ratio $(2a/L)$ of the cavity keeping in mind that the HTS thin films are usually deposited on a 10 mm $\times$ 10 mm substrate. In this discussion, we consider the following three cases:

1) complete end-plate substitution of the TE_{011}-mode cavity by a sample of size 9.6-mm diameter;
2) partial end-plate substitution in which a sample of 9.6-mm diameter concentrically substitute a portion of the end plate of the TE_{011}-mode cavity operating at 20 GHz;
3) laterally resolved R_s measurement of the HTS sample by exposing different area of the sample to microwaves inside the cavity operating at 20 GHz.

The measurement sensitivity of any resonant technique is primarily determined by the Q value of the resonant structure and is directly related to the dynamic range of the Q value for the change in $R_{ssample}$. The sensitivity of the measurement by the cavity end-plate substitution technique depends on the aspect ratio $2a/L$, size of the sample, and surface resistance of the walls of the cavity. One can expect that with a decrease in the surface resistance of the sample, the Q value of the cavity will increase proportionally and $R_{\rm ssample}$ can easily be calculated from the measured difference in the Q values of the cavity with and without the sample. However, it is not the case; actually, the Q value of the cavity with a sample will increase only up to a certain low value of $R_{\rm ssample}$ and, thereafter, it will tend to saturate since the relative ohmic loss in the metallic part of the cavity dominates and solely decides the Q value. The Q value saturates to a $Q_{\max}$ value, i.e., the Q value of the cavity with a lossless sample and can be expressed by substituting $R_{\rm ssample} = 0$ in (8) as

$$\frac{1}{Q_{\max}} = \left[\left\{\frac{1}{G} - \frac{1}{S(d)}\right\} R_{scu}\right]. \tag{13}$$

The $Q_{\max}$ value depends on the geometrical factors of the cavity and the sample, R_{scu} and the mode of the cavity. The dependence of the dynamic range of the Q value for the change in $R_{\rm ssample}$ is reflected in the behavior of $|Q_{os} - Q_{oc}|/Q_{oc}$ as a function of $R_{\rm ssample}/R_{scu}$. Similar to the above discussion, $|Q_{os} - Q_{oc}|/Q_{oc}$ initially increases and tend to saturate to a value $F(d)$, which is defined as the figure-of-merit of the measurement [15], which can be expressed as

$$F(d) = |Q_{\max} - Q_{oc}|/Q_{oc}. \tag{14}$$

Increase in the value of $F(d)$ means an increase in the sensitivity of the measurement, as for a large value of $F(d)$, saturation in $|Q_{os} - Q_{oc}|/Q_{oc}$ starts at the lower value of the $R_{\rm ssample}$, which gives better dynamic range of the Q value of the cavity for the change in the R_s value of the sample [9], [15]. This will become clearer as we discuss the specific case.

A. Complete End-Plate Substitution Technique

Considering the case of R_s measurement of HTS thin films deposited on a 10 mm $\times$ 10 mm substrate, we evaluated $|Q_{os} - Q_{oc}|/Q_{oc}$ as a function of $R_{\rm ssample}/R_{scu}$ for a sample of a fixed diameter of 9.6 mm, which completely substitutes the end plate of the cavity. The analysis of a mode chart for cylindrical cavities [16] shows that for the square of aspect ratios (SAR's) in the range of $(2a/L)^2 = 2$ to $(2a/L)^2 = 4.25$, other modes are out of the vicinity of the $\rm TE_{011}$ mode. Fig. 2 shows the calculated $|Q_{os} - Q_{oc}|/Q_{oc}$ as a function of $R_{\rm ssample}/R_{scu}$ for a fixed cavity diameter ($2a = 9.6$ mm) and R_{scu} value (at 77 K) for the range of the SAR, $2 \leq \rm SAR \leq 4.25$. It shows that $|Q_{os} - Q_{oc}|/Q_{oc}$ increases as $R_{\rm ssample}$ decreases and tends to saturate to a value $F(d)$ at a lower value of $R_{\rm ssample}$ with an increasing SAR. This, in fact, is due to the decrease in the loss contribution by the lateral walls of the cavity with the decrease in the length of the cavity. Saturation occurs at lower $R_{\rm ssample}$ for a larger value of $F(d)$, giving larger dynamic range in Q value and, therefore, more sensitive measurement. The ultimate measurement sensitivity will depend on the observable change in Q value with a fractional change in $R_{\rm ssample}$ and can be roughly estimated by the point of intersection of the tangents drawn on the curve shown in Fig. 2. Table I shows the computed Q values of cavity, geometrical factors, $F(d)$, and sensitivity for different SAR value. The inset in Fig. 2 shows the plot of $F(d)$ as a function of the SAR. It shows that highest sensitivity is achieved for

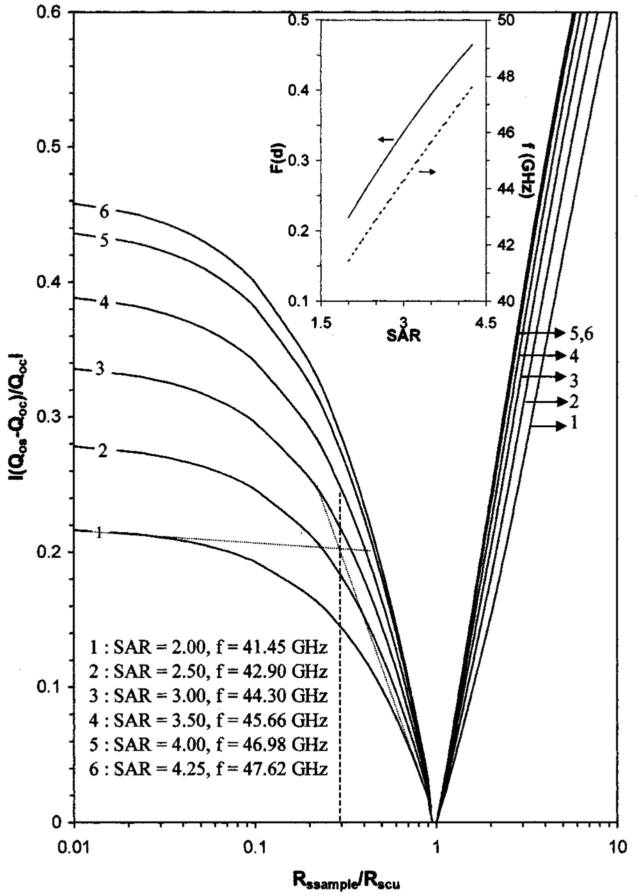

Fig. 2. Theoretically computed normalized change in the Q value $|Q_{os} - Q_{oc}|/Q_{oc}$ as a function of $R_{\rm ssample}/R_{scu}$ for a cavity of 9.6-mm diameter for the range of the SAR $2 \leq \rm SAR \leq 4.25$. The inset shows the change in $F(d)$ and resonant frequency f_0 as a function of the SAR.

the largest value of SAR (=4.25), which, for a 9.6-mm diameter cavity, gives the resonance frequency of a $\rm TE_{011}$ mode at 47.62 GHz. However, this is at the cost of Q_{oc} and $Q_{\max}$ values (see Table I). Q_{oc} decreases significantly for $(2a/L)^2 = 4.25$, hence, one needs to compromise in selecting the value of the aspect ratio and maintain a balance between Q values and $F(d)$. Thus, for the $\rm TE_{011}$ mode of a 9.6-mm-diameter cavity, maximum value of the SAR would yield a maximum sensitivity limit of 13% of the R_{scu} value for a single end-plate substitution.

The practical application for HTS microwave devices has been identified in the frequency range of 1–20 GHz. According to the two-fluid model [17], R_s of superconductors scales quadratic with frequency ($R_s \propto \omega^2$). Experimentally, it has been observed [18] that the exponent α of $R_s \propto \omega^\alpha$ need not necessarily be "2" for the HTS, rather it lies in the range of 1.2–1.7. It is, therefore, desirable to measure the characteristics of the HTS by the system operating at the frequency of interest.

B. Partial End-Plate Substitution Technique

Using a cavity resonator the R_s measurement of HTS thin films (10 mm $\times$ 10 mm) at low frequencies can be made by a partial end-plate substitution technique. In this method, the sample is embedded at the center of the end plate of the cavity and has a circularly symmetric exposure to microwaves using an

TABLE I
THEORETICALLY CALCULATED PARAMETERS FOR COMPLETE ENDPLATE SUBSTITUTION TECHNIQUE FOR SAMPLE AT 77 K
(DIAMETER OF THE SAMPLE = 9.6 mm)

SAR $(2a/L)^2$	f GHz	Geom. factor of cavity (G) 'Ω'	Geom. factor of endplate S(d) 'Ω'	Loss from single end wall (%)	Q-value of the copper cavity Q_{oc}	Maximum Q-value Q_{max}	Figure of merit F(d)	Sensitivity $R_{ssample}/R_{scu}$ (%)
2.00	41.45	763.2	4248	17.97	20628.04	25145.75	0.219008	30
2.25	42.18	751.9	3749	20.06	20145.99	25200.14	0.250876	28
2.50	42.90	740.13	3367	21.98	19663.52	25203.79	0.281754	25
2.75	43.61	728.05	3065	23.75	19184.48	25161.19	0.311539	22
3.00	44.30	715.97	2820	25.39	18718.66	25088.35	0.340285	20
3.25	44.98	704.03	2619	26.88	18266.84	24982.55	0.367645	18
3.50	45.66	692.36	2450	28.26	17829.78	24853.18	0.393915	16
3.75	46.32	681.02	2307	29.52	17412.35	24705.28	0.418837	15
4.00	46.98	670.07	2184	30.68	17011.61	24541.01	0.442603	14
4.25	47.62	659.54	2078	31.74	16631.38	24364.46	0.464969	13

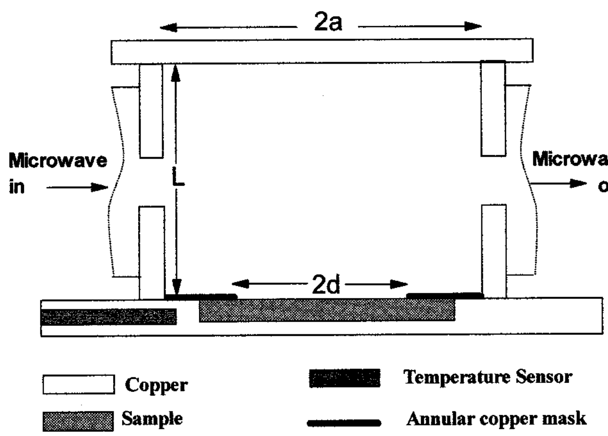

Fig. 3. Schematic diagram of partial end-plate substitution technique in a cylindrical copper cavity.

annular laminar mask (opening diameter $= 2d$) on top of it, as shown in Fig. 3. We considered the opening diameter of 9.6 mm for the HTS thin films deposited on a 10 mm × 10 mm substrate to prevent exposure of the edges of the thin film. Fig. 4 shows the variation of $|Q_{os}-Q_{oc}|/Q_{oc}$ as a function of $R_{\rm ssample}/R_{scu}$ for $2 \le \mathrm{SAR} \le 4.25$ at 20 GHz for the sample of fixed diameter $2d = 9.6$ mm. It shows that $|Q_{os} - Q_{oc}|/Q_{oc}$ increases as $R_{\rm ssample}$ decreases and tends to saturate at lower $R_{\rm ssample}$ with an increase in the SAR value up to 3.5. Further increase in the SAR reverses the trend and saturation begins at a higher value of $R_{\rm ssample}$. The inset in Fig. 4 shows a peak in $F(d)$ near the $\mathrm{SAR} = 3.0$, suggesting maximum measurement sensitivity, although the dynamic range of the Q value of the cavity for change in the R_s value of the sample is almost the same for the SAR between 3–4.25. The difference between the behavior of $F(d)$ in the complete end-plate substitution technique (inset of Fig. 2) and this technique is due to the $Q_{\max}$ value that depends on the loss contribution by the sample area in the total

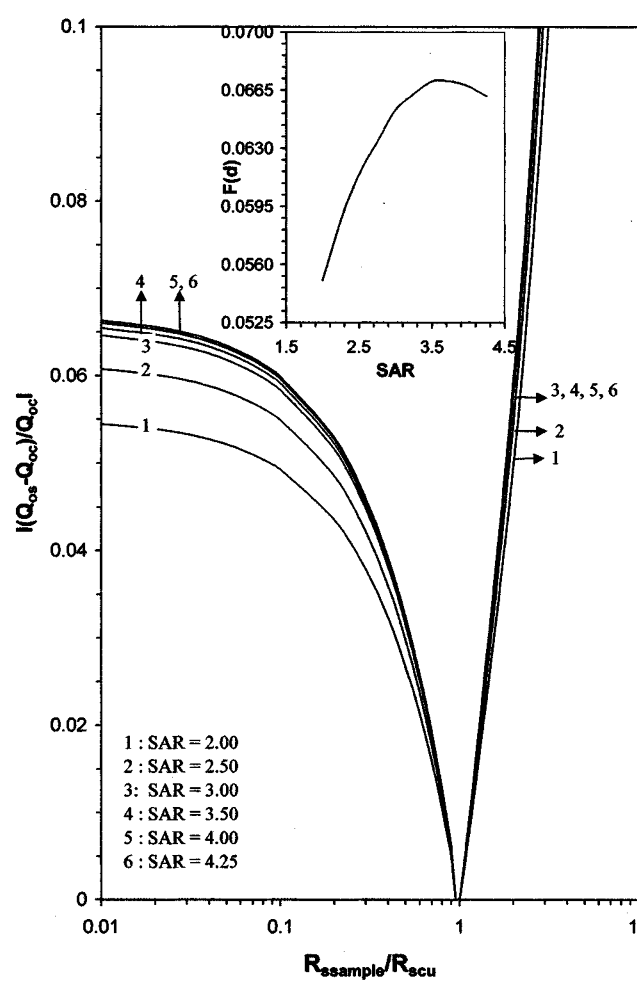

Fig. 4. Theoretically computed normalized change in the Q value $|Q_{os} - Q_{oc}|/Q_{oc}$ as a function of $R_{ssample}/R_{scu}$ for $2 \le \mathrm{SAR} \le 4.25$ at 20 GHz for the sample of fixed diameter $2d = 9.6$ mm. The inset shows the change in $F(d)$ as a function of the SAR.

TABLE II
THEORETICALLY CALCULATED PARAMETERS FOR PARTIAL ENDPLATE SUBSTITUTION TECHNIQUE IN A 20-GHz CAVITY AT 77 K (DIAMETER OF THE SAMPLE $(2d) = 9.6$ mm)

SAR $(2a/L)^2$	Diameter of cavity '2a' mm	Geom. factor of cavity (G) 'Ω'	Geom. factor of sample S(d) 'Ω'	Loss from sample portion (%)	Q-value of copper cavity Q_{oc}	Maximum Q-value Q_{max}	Figure of merit F(d)	Sensitivity $R_{ssample}/R_{scu}$ (%)
2.00	21.10	763.17	14630	5.22	29695.33	31329.63	0.05503	45
2.25	21.50	751.94	13570	5.54	29258.37	30974.74	0.05866	42
2.50	21.79	740.13	12790	5.79	28798.83	30567.72	0.06142	40
2.75	22.14	728.06	12210	5.96	28329.18	30125.51	0.06340	39
3.00	22.42	715.97	11680	6.13	27858.75	29677.98	0.06530	38
3.25	22.75	704.03	11350	6.20	27394.16	29205.77	0.06613	37
3.50	23.02	692.35	11020	6.28	26939.69	28745.68	0.06703	35
3.75	23.35	681.02	10840	6.28	26498.83	28275.22	0.06703	35
4.00	23.66	670.07	10710	6.26	26072.76	27812.87	0.06674	36
4.25	23.98	659.54	10630	6.20	25663.04	27360.63	0.06614	37

conductive losses of the cavity. In the case of complete end-plate substitution, the contribution of the end plate in the total conductive loss of the cavity increases with an increase in the SAR, giving a monotonic increase in the $Q_{\max}$ value. Whereas in the partial end-plate substitution technique, the sample only substitutes a central part of the end plate and, therefore, the loss contribution by the sample portion also depends on the current distribution at the end plate, as shown in Table II. For the TE_{011} mode, the region of maximum current density at the end plate lies nearly half of the radial distance from the center, and the loss contribution by the sample area will significantly depends on the coverage of this region by it. In this particular case of a cavity operating at 20 GHz with $2d = 9.6$ mm, the difference in Q values (i.e., $Q_{\max} - Q_{oc}$) increases with increase in cavity diameter $(2a)$ up to the value of 23 mm (for $\mathrm{SAR} = 3.5$) due to an increase in the loss contribution by the sample part resulting from the increasing strength of the current in the end plate and, hence, in the sample area. Further increase in the diameter of the end plate moves the region of maximum current density away from its center, and that reduces the coverage of the maximum current region in the sample area, resulting in lowering the $(Q_{\max} - Q_{oc})$ value. The analysis suggests that, for the cavity under consideration $2a = 22.42$ mm and $\mathrm{SAR} = 3$ will provide a maximum sensitivity limit (38% of R_{scu} value) with an optimum Q_{oc} value.

C. Laterally Resolved R_s Measurement

Laterally resolved R_s measurement of the HTS sample can be done by exposing the different areas of the sample to microwaves through laminar masks of different openings inside the cavity, as shown in Fig. 4. However, by exposing sample areas that are smaller than the cavity diameter, the sensitivity is reduced due to the fact that a smaller percentage of the total cavity surface area has been replaced compared to the complete end-plate substitution. Fig. 5 shows calculations of $|Q_{os} - Q_{oc}/Q_{oc}$ as a function of $R_{\mathrm{ssample}}/R_{scu}$ for the different areas of the sample $(2d)$ exposed to microwaves inside cavity operating at

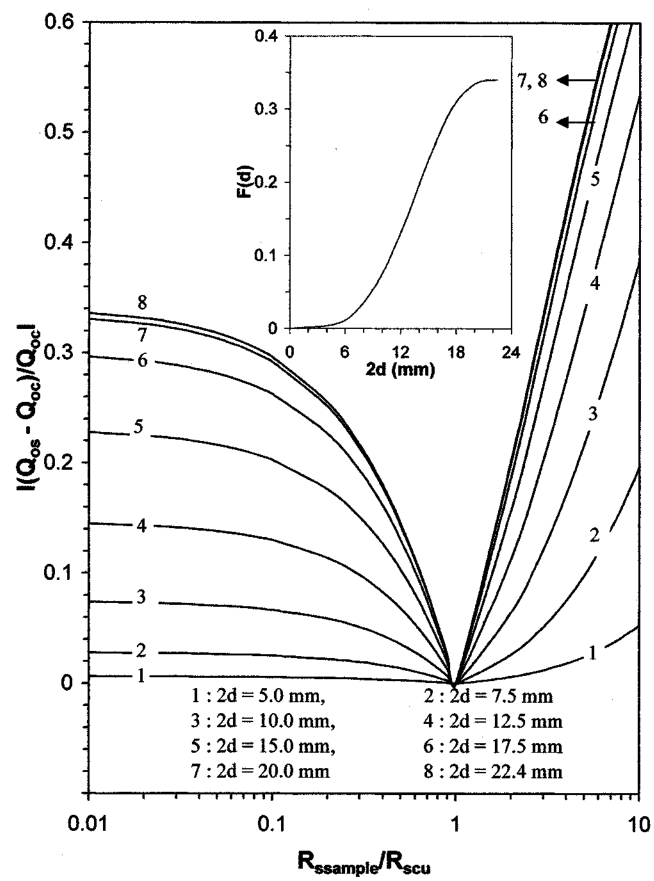

Fig. 5. Theoretically computed normalized change in the Q value $|Q_{os} - Q_{oc}|/Q_{oc}$ as a function of $R_{\mathrm{ssample}}/R_{scu}$ for different areas of a sample exposed to microwaves inside the cavity The inset shows the change in $F(d)$ as a function of the area of the sample exposed to microwaves inside the cavity.

TABLE III
THEORETICALLY CALCULATED PARAMETERS FOR LATERALLY RESOLVED SURFACE-RESISTANCE MEASUREMENT BY PARTIAL ENDPLATE SUBSTITUTION TECHNIQUE IN A 20-GHz CAVITY AT 77 K ($Q_{oc} = 27860$, $G = 716\ \Omega$)

Sample diameter '2d' mm	Geom. factor of sample S(d) 'Ω'	Loss from sample portion (%)	Maximum Q-value Q_{max}	Figure of merit F(d)	Sensitivity $R_{ssample}/R_{scu}$ (%)
2.5	1.61×10^{10}	0	27859.92	0	100
5.0	113800	0.629	28036.32	0.0063	76
7.5	26220	2.731	28642.06	0.0281	60
10.0	10310	6.945	29939.11	0.0746	38
12.5	5602	12.781	31942.55	0.1465	32
15.0	3822	18.734	34282.24	0.2305	27
17.5	3099	23.104	36230.76	0.3005	22
20.0	2853	25.096	37194.36	0.3350	20
22.4	2819	25.399	37345.28	0.3405	20

20 GHz and having dimensions $2a = 22.4$ mm, $L = 12.94$ mm with $R_{scu} = 25.7\ \text{m}\Omega$ (at 20 GHz and 77K). It shows that $|Q_{os} - Q_{oc}|/Q_{oc}$ increases as R_{ssample} decreases and saturates at the lower R_{ssample} value with an increase in the exposed area of the sample due to increase in the loss contribution by the sample. It is to be noted that the saturation value of $|Q_{os} - Q_{oc}|/Q_{oc}$ increases appreciably for the exposed area having the radius approximately greater than half of the radius of the end plate, which is due to the increment in the coverage of the maximum current area by the sample, as shown in Table III. As seen from the table, the maximum sensitivity limit, as expected, would be achieved for the complete end-plate substitution and decreases as the area of the sample exposed to microwaves decreases. It also shows that, for the sample area $\leq$5.0-mm diameter, the loss contribution by the sample is almost negligible and it is not possible to observe change in the Q value due to the sample. However, Wosik *et al.* [15] reported the measurement of YBCO single crystals of 2.0-mm-diameter size by the partial end-plate substitution technique, but the cavity used for measurement was operated at 80 GHz.

V. EXPERIMENTAL

Considering the R_s measurement of 10 mm $\times$ 10 mm HTS thin films, we selected the dimensions of the TE_{011}-mode 20-GHz cavity as $2a = 22.42$ mm and $L = 12.94$ mm for $(2a/L)^2 = 3$. The cavity is fabricated in three modules, the circular top plate, cylindrical, and a circular base plate having the same dimensions as the cold finger platform (40 mm). All parts of cavity are well polished and then silver plated to improve the surface smoothness. A mode trap in the form of a groove in the top plate is designed to shift the degenerate TM_{111} mode to a lower frequency. Microwave power coupling is achieved by SMA to waveguide adapter connection through diametrically opposite iris holes, of diameter 3.5 mm, at the center of the lateral wall of the cavity. The waveguide couples to the magnetic field of the resonant mode of the cavity through iris holes.

Measurements were carried out by complete end-plate substitution for YBCO bulk samples (25-mm diameter), prepared by the conventional solid-state technique, and for Ag-doped YBCO thin films on $LaAlO_3$ (10 mm $\times$ 10 mm) substrate prepared by pulsed laser deposition technique [19] by partial end-plate substitution. The dc transition temperatures of the samples were around 90 K. The thin film was embedded in the bottom end plate of the cavity and silver-coated copper mask of 9.6-mm inner diameter was properly placed on top of it, as shown in Fig. 3. At the TE_{011} mode, the microwave current flows along the surface of the sample and there is no penetration of the microwave field from the edges of the mask. The annular mask through which the sample was exposed to microwaves also acts as a mode trap. The mask was properly aligned to maintain concentricity inside the cavity and to avoid any air gap to prevent microwave leakage. The whole assembly after loading on the cryo-cooler was enclosed in a glass dome and evacuated before pumping to reduce the temperature. Microwaves to the resonator are swept using an HP 8350 sweeper with an HP 83595 plug-in and the transmitter output is analyzed by an HP 8757D scalar network analyzer. The unloaded Q value of the resonator is obtained using the relation

$$Q_o = Q_L[1 - 10^{-(IL/20)}]^{-1}$$

where Q_L is the measured loaded Q value $(f_0/\Delta f)$ and IL is the insertion loss (in decibels) at the resonance frequency f_0 in the transmission mode, and Δf is the measured 3-dB bandwidth. The characteristic parameters were measured in the temperature range of 20–100 K recorded by a calibrated carbon glass resistance (CGR) temperature sensor fixed in the vicinity of the sample. To minimize error in the temperature measurements, an indium sheet has been used at the cold finger–cavity interface. The laterally resolved surface resistance measurements of the bulk and thin-film samples were carried out by exposing the sample to the microwaves through silver-coated copper laminar masks of different inner diameters. In addition, the cavity is carefully calibrated, with each mask, at each temperature point.

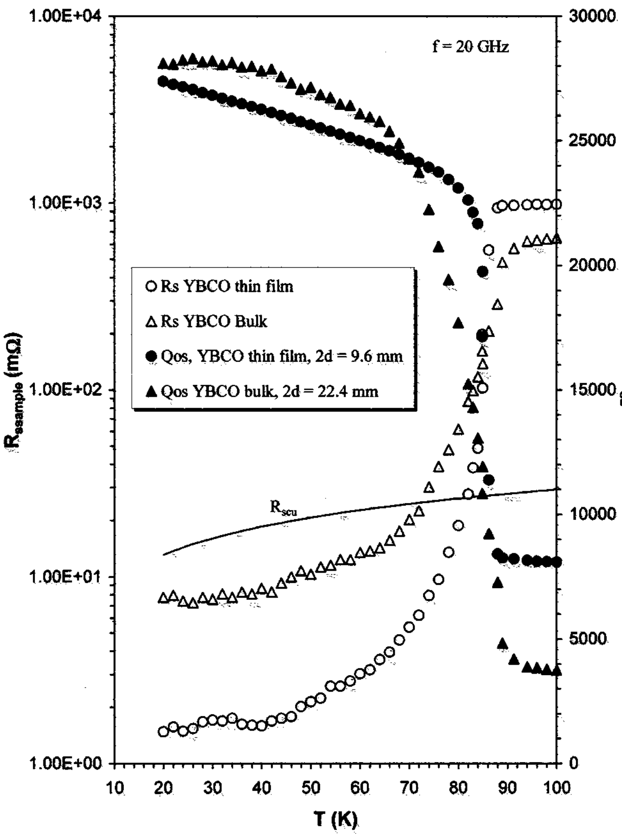

Fig. 6. Measured unloaded Q value Q_{os} and deduced surface resistance $R_{ssample}$ of a YBCO bulk sample completely substituting the end plate and that of a YBCO thin film substituting 9.6 mm of the cavity end plate, as a function of temperature at 20 GHz.

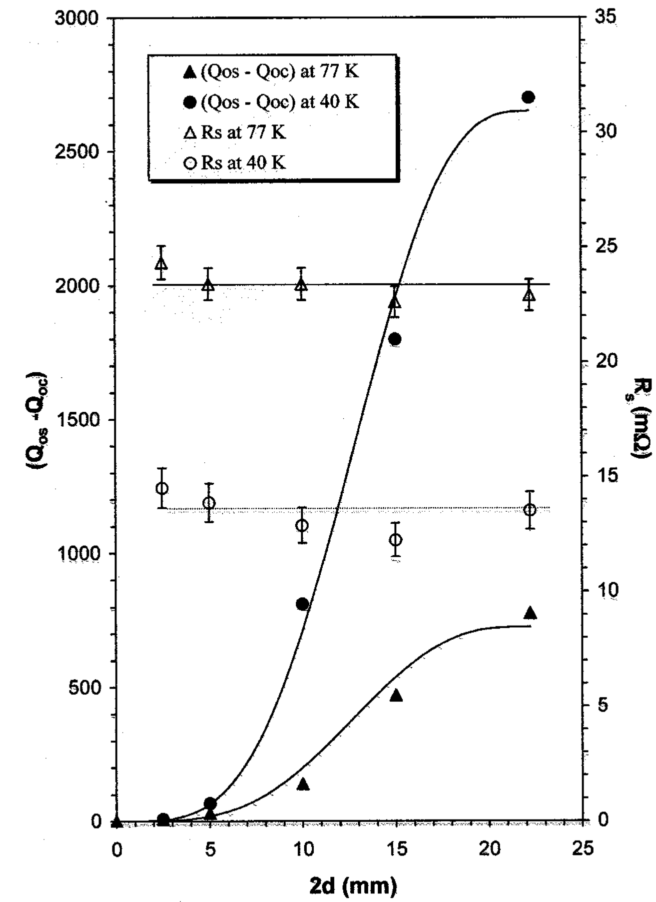

Fig. 7. Measured variation of $(Q_{os} - Q_{oc})$ and deduced surface resistance of a YBCO bulk sample with a different area of the sample exposed to microwaves inside the cavity at temperatures 77 and 40 K and frequency 20 GHz.

VI. Results and Discussion

Fig. 6 displays the typical temperature variation of the measured Q value and the extracted surface resistance R_{ssample} for a YBCO bulk sample and a thin film at 20 GHz and in the temperature range of 20–100 K. The bulk sample completely substituted the end plate of the cavity, whereas the thin film was measured by exposing it to microwaves through a laminar mask of 9.6-mm diameter. Both samples show a monotonic behavior above T_c. The T_c onset and transition width measured from the $R_s\,(T)$ behavior is almost the same as that measured by susceptibility measurements. In the region below T_c, the relative changes in R_s decrease and saturate to a finite residual value although the transition width of the bulk sample is relatively higher than that of the thin film. The surface resistance of the bulk sample is 23.1 $\text{m}\cdot\Omega$ at 77 K and 20 GHz. This value of R_s corresponds to 5.77 mΩ at 10 GHz assuming quadratic frequency dependence of R_s and is comparable to the best-reported value in a polycrystalline bulk sample. In the case of a thin film near the superconducting transition $(T < T_c)$, R_s decreases sharply down to the temperature 55 K due to the rapid condensation of the normal electrons into superconducting state. Between the temperatures of 55 and 40 K, R_s decreases slowly, which is attributed to an increase in the mean free path of quasi-particles or corresponding reduction in the quasi-particle scattering rate at around $T_c/2$ [20]. The lowest value measured is 1.6 mΩ at 20 K. The measured sensitivity is important below the crossover temperature where R_{ssample} is lower than the R_{scu} value, which, for the bulk sample, is 74 K and that of thin film is 84 K.

Fig. 7 shows the change in the unloaded Q value of the cavity containing a bulk YBCO sample and the extracted R_s value of the sample as a function of the area of the sample exposed to the microwave inside cavity through laminar masks having different inner diameters. The laterally resolved R_s values of the sample ranges between (23.7±1 mΩ) at 77 K and (14±1 mΩ) at 40 K. Fig. 8 shows the change in the unloaded Q value of the cavity containing a thin film with respect to that of the cavity containing a copper sample and the extracted R_s value of the sample at temperatures 77 and 40 K as a function of the area of the sample exposed to the microwaves inside the cavity through annular masks having inner diameters 5.0, 7.5, and 9.6 mm. The laterally resolved R_s values of the sample for different exposed area ranges between (1.6±0.12 mΩ) at 40 K and (9.6±0.2 mΩ) at 77 K. The relative measurement variation in the case of bulk sample is more than that of a thin film, which can be expected since the film surface is smoother than that of the bulk sample.

Resonators are based on the idea that the change in the resonant frequency can be related to the imaginary part of the surface impedance, i.e., the surface reactance X_s [21]. In superconductors, X_s is directly proportional to the magnetic penetration depth λ. Measurement of λ using the end-plate substitution technique has also been reported [6] in some cases. However,

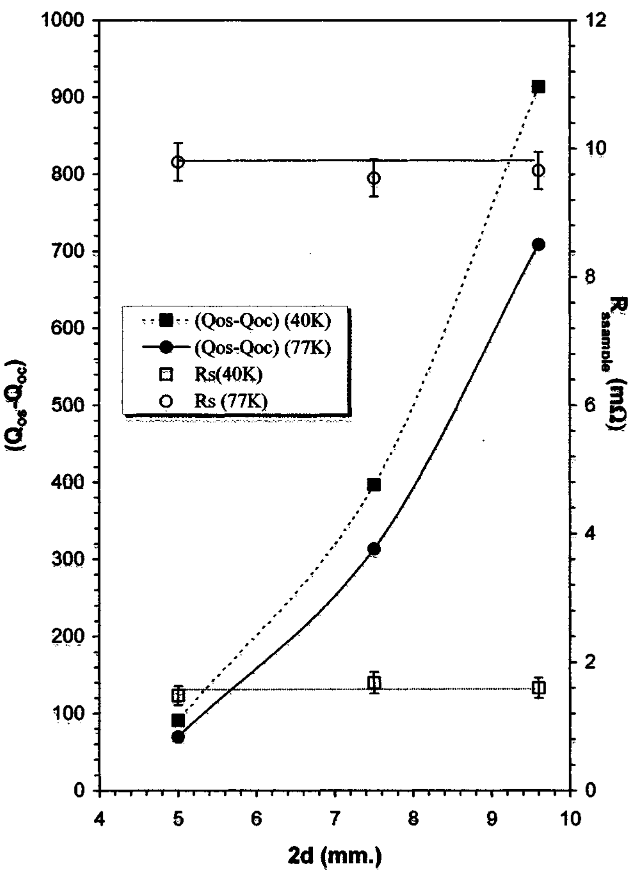

Fig. 8. Measured variation of $(Q_{os} - Q_{oc})$ and deduced surface resistance of a YBCO thin film with a different area of the sample exposed to microwaves inside the cavity at temperatures 77 and 40 K and frequency 20 GHz.

it is pertinent that the change in frequency due to the size effect and change in conductivity of the material of cavity be subtracted to extract the change due to the sample. In the end-plate substitution technique, the observed change in frequency could not determine the temperature dependence of λ since the change in frequency due to background is more pronounced. Therefore, the measurement of X_s could not be included.

The sensitivity of measurement, by complete end-plate substitution or partial substitution technique can be improved by: 1) increasing $F(d)$, which depends on the loss contribution by the sample portion and 2) using cavities made of superconducting materials, which increases the $Q_{\max}$ value, and sensitivity improves due to the lower $R_{scavity}$ value in the ratio $R_{ssample}/R_{scavity}$. Substituting both the end plates of the cavity by test samples having similar $R_{ssample}$ values would improve the measurement sensitivity. Taking the 20-GHz cavity, as discussed above, and completely substituting both the end plates by samples the estimated $F(d)$ is 1.03, which shows a significant improvement over the case where only one end plate of the cavity is completely substituted by the sample. Another possibility is to use higher modes of the cavity, e.g., TE_{012}, TE_{013}, for which the conductive losses in the end plate of the cavity are more significant than those for the TE_{011} mode [15]. Also, in a right cylindrical cavity, the Q value of the TM_{011} mode is more sensitive to the surface resistance of the end plate than that for the TE_{011} mode [22]. However, the selection of the TM_{011} mode for the measurement of surface resistance by an end-plate substitution method is restricted due to the strong radial currents crossing the end wall–cavity interface. However, using TE_{011} mode does not allow characterizing the materials as a function of the external magnetic field.

The other way of improving the sensitivity of measurement is by replacing the copper cavity by a superconducting niobium cavity whose surface resistance is much smaller than that of copper. Considering the geometry of the cavity under discussion having a sensitivity of measuring $R_{ssample}$ up to 20% of the $R_{scavity}$ value will give the measurable limit of 5 $\mu\Omega$ of $R_{ssample}$ with the dynamic range of the Q value $(Q_{max} - Q_{oc})$ of 9.8 × 10^6 for superconducting niobium cavity with $R_{sNb} = 25\,\mu\Omega$ at 4.2 K and 20 GHz. The disadvantage of using all of the Nb cavity for end-plate substitution is that the measurement of $R_{ssample}$ can be made only at or below T_c of niobium, i.e., below 9.2 K. However, Sridhar and Kennedy have made measurements of $R_{ssample}$ to higher temperatures using an Nb cavity through a different approach, i.e., the cavity perturbation technique [7]. The technique allows variation in the temperature of the sample while maintaining the constant cavity temperature (4.2 K). However, the measurement is limited only to small-sized samples. Alternately, an all-HTS cavity can be fabricated either from a bulk HTS cylinder or coating thick or thin films on the walls of a supporting substrate material [23]. The measurement sensitivity in the case of end-plate substitution would be improved provided the $R_{ssample}$ value is lower than that of the host cavity so that the measured difference in the Q value is measurable.

VII. Conclusion

An expression for the Q value of the TE_{011} cavity has been derived as a function of the dimensions of the sample substituted in the end wall of the cavity by solving the electromagnetic-field equations using boundary conditions. This facilitates the laterally resolved R_s measurement of the HTS samples. The sensitivity of the measurement is evaluated for the case of complete end-plate substitution as well as partial end-plate substitution. A cylindrical TE_{011} mode copper cavity is designed and fabricated to measure the surface resistance of bulk and thin films of an HTS at 20 GHz by selecting the dimensions that yields maximum sensitivity for measurement of 10 mm × 10 mm samples. The result of the analysis shows that complete end-plate substitution yields sensitivity limit of 20% of R_{scu} value. As the size of the sample is reduced, the loss contribution by the sample to the total cavity losses reduces and, consequently, the limit of sensitivity increases; for the samples of dimensions less than a 5.0-mm diameter, it becomes impossible to accurately determine the R_s value of the sample within the possible measurements error.

Appendix
Derivation of the Unloaded Q-Value of the Cylindrical Cavity Resonator for the Partial End-Plate Substitution of the Sample

The total energy W_t stored inside the cavity can be expressed as

$$W_t = \frac{1}{2}\,\varepsilon \int_{\text{cavity}} \left|\overline{E}_\phi\right|^2 dV \tag{A1}$$

$$\frac{1}{Q_{os}} = \frac{1}{2\pi}\,\frac{2\pi}{C}\,(\alpha_1^2+\alpha_2^2)^{-1/2}\left[\frac{\frac{1}{2}\,\pi\alpha_2^2 J_0^2(\alpha_2 a)\left[a^2\alpha_1^2 R_{st} + aL\alpha_2^2 R_{ss} + d^2\alpha_1^2\eta(d)R_{\text{ssample}} + d^2\alpha_1^2\left\{\frac{a^2}{d^2}-\eta(d)\right\}R_{sb}\right]}{\frac{1}{4}\,\pi\mu a^2 L\alpha_2^2(\alpha_1^2+\alpha_2^2)J_0^2(\alpha_2 a)}\right] \tag{A7}$$

using (4a) and integrating using boundary conditions

$$W_t = \frac{1}{2}\,\mu(\alpha_1^2+\alpha_2^2)\alpha_2^2\left[\int_{\rho=0}^{\rho=a} J_0'^2(\alpha_2\rho)\rho\,d\rho \cdot \int_{z=0}^{z=L}\sin^2(\alpha_1 z)\,dz\int_{\phi=0}^{\phi=2\pi} d\phi\right]$$

$$W_t = \frac{1}{4}\,\mu\pi a^2 L(\alpha_1^2+\alpha_2^2)\alpha_2^2 J_0^2(\alpha_2 a). \tag{A2}$$

In a hollow cavity resonator, power dissipates only due to the conduction loss that results from the finite conductivity of the cavity walls and that of the superconductor sample. The total power dissipation P_l in the cavity is expressed as the power dissipation in the walls of the top end plate P_t, sidewalls P_s, metallic portion of the bottom end plate P_{bm}, and the sample P_{bs} as

$$P_l = P_t + P_s + P_{bm} + P_{bs}. \tag{A3}$$

The conductive power loss in the various parts of the cavity can be obtained by using (2) and (4) with proper boundary conditions as

$$\begin{aligned} P_l = &\frac{1}{2}\,R_{st}\alpha_1^2\alpha_2^2\left[\int_{\rho=0}^{\rho=a} J_0'^2(\alpha_2\rho)\rho\,d\rho\int_{\phi=0}^{\phi=2\pi} d\phi\right] \\ &+\frac{1}{2}\,R_{ss}\alpha_2^4 J_0^2(\alpha_2 a)\left[\int_{\rho=0}^{\rho=a} d\rho\int_{z=0}^{z=L}\sin^2(\alpha_1 z)\,dz \cdot\int_{\phi=0}^{\phi=2\pi} d\phi\right] \\ &+\frac{1}{2}\,R_{sb}\left[\int_{\rho=d}^{\rho=a} J_0'^2(\alpha_2\rho)\rho\,d\rho\int_{\phi=0}^{\phi=2\pi} d\phi\right] \\ &+\frac{1}{2}\,R_{\text{ssample}}\alpha_1^2\alpha_2^2\left[\int_{\rho=0}^{\rho=d} J_0'^2(\alpha_2\rho)\rho\,d\rho\int_{\phi=0}^{\phi=2\pi} d\phi\right] \end{aligned} \tag{A4}$$

where R_{st}, R_{ss}, and R_{sb} are the surface resistance values of material of the top plate, sidewalls, and bottom plate of the cavity, and R_{ssample} is the surface resistance of the sample substituting the bottom end plate of the cavity. The solution of (A4) yields

$$P_l = \frac{1}{2}\,\pi\alpha_2^2 J_0^2(\alpha_2 a)\left[a^2\alpha_1^2 R_{st} + aL\alpha_2^2 R_{ss} + d^2\alpha_1^2 \cdot\left\{\frac{a^2}{d^2}-\eta(d)\right\}R_{sb} + d^2\alpha_1^2\eta(d)R_{\text{ssample}}\right] \tag{A5}$$

where

$$\eta(d) = \left[\frac{J_1^2(\alpha_2 d)}{J_0^2(\alpha_2 a)}\left\{1-\frac{2}{\alpha_2 d}\,\frac{J_0(\alpha_2 d)}{J_1(\alpha_2 d)}\right\}+\frac{J_0^2(\alpha_2 d)}{J_0^2(\alpha_2 a)}\right]. \tag{A6}$$

Substituting the values of W_t and P_l from (A2) and (A5) in (1), the unloaded Q value of the cavity containing the sample Q value can be expressed as shown in (A7), at the top of this page. Solving (A7) yields

$$\frac{1}{Q_{os}} = \frac{2}{Z_0}\,\frac{1}{a^2 L}\,\frac{1}{(\alpha_1^2+\alpha_2^2)^{3/2}} \cdot\left[a^2\alpha_1^2 R_{st} + aL\alpha_2^2 R_{ss} + d^2\alpha_1^2\eta(d)R_{\text{ssample}} + d^2\alpha_1^2\left\{\frac{a^2}{d^2}-\eta(d)\right\}R_{sb}\right] \tag{A8}$$

where $Z_0 = \sqrt{\mu_0/\varepsilon_0}$ is the impedance of free space.

Acknowledgment

The authors would like to thank Prof. A. K. Raychaudhuri, Director, National Physical Laboratory, New Delhi, India, for his encouragement and Prof. R. Pinto, Tata Institute of Fundamental Research (TIFR), Mumbai, India, for providing YBCO thin film.

References

[1] A. B. Pippard, “An experimental and theoretical study of relation between magnetic field and current in superconductor,” *Proc. R. Soc. Lond. A, Math. Astron. Phys. Sci.*, vol. A216, pp. 547–568, 1953.
[2] N. D. Kataria, M. Jaya Kumar, and G. P. Srivastava, “Microwave surface impedance of high temperature superconductors and device applications,” in *Studies of High Temperature Superconductors*, A. V. Narlikar, Ed. New York: Nova Sci., 1996, vol. 18, pp. 45–100.
[3] R. C. Taber, “A parallel plate resonator technique for microwave loss measurements of superconductors,” *Rev. Sci. Instrum.*, vol. 61, pp. 2200–2206, 1990.
[4] J. Krupka, M. Klinger, M. Kuhn, A. Baranyak, M. Steller, J. Hinken, and J. Modelski, “Surface resistance measurements of HTS films by means of sapphire dielectric resonators,” *IEEE Trans. Appl. Superconduct.*, vol. 3, pp. 3043–3048, Sept. 1993.
[5] D. E. Oates and A. C. Anderson, “Surface impedance measurements of YBaCuO thin films in stripline resonators,” *IEEE Trans. Magn.*, vol. 27, pp. 867–871, Mar. 1991.
[6] B. A. Tonkin and Y. G. Proykova, “Modular system for microwave surface impedance measurement of high-temperature superconductors,” *Superconduct. Sci. Technol.*, vol. 6, pp. 353–359, 1993.
[7] S. Sridhar and W. L. Kennedy, “Novel technique to measure the microwave response of high T_c superconductors between 4.2 and 200K,” *Rev. Sci. Instrum.*, vol. 59, pp. 531–536, 1988.
[8] M. Jayakumar, N. D. Kataria, and G. P. Srivastava, “10-GHz cylindrical cavity resonator for characterization of high-T_c superconducting bulk and thin films,” *IEEE Trans. Magn.*, vol. 30, pp. 4605–4607, Nov. 1994.
[9] M. Misra, N. D. Kataria, and G. P. Srivastava, “Sensitivity in the measurement of microwave surface resistance of high-T_c superconducting samples of different size by cavity method,” *Supercond. Sci. Technol.*, vol. 12, pp. 48–53, 1999.

[10] E. Silva, M. Lancura, and R. Marcon, "Microwave surface resistance peak at T_c in $Bi_2Sr_2CaCu_2O_{8+x}$ film," *Physica C*, vol. 276, pp. 84–90, 1997.
[11] L. Hao and J. C. Gallop, "Spatially resolved measurements of HTS microwave surface impedance," *IEEE Trans. Appl. Superconduct.*, vol. 9, pp. 1944–1947, May 1999.
[12] E. Argence and T. Kahan, "Electromagnetic cavities," in *Theory of Waveguides and Cavity Resonators*. Glasgow, Scotland: Blackie, 1967, pp. 361–372.
[13] N. Klein, H. Chaloupka, G. Muller, S. Orbach, H. Piel, B. Roas, L. Schultz, U. Klien, and M. Peiniger, "The effective microwave surface impedance of epitaxial $YBa_2Cu_3O_{7-\delta}$ thin films," *J. Appl. Phys.*, vol. 67, pp. 6940–6945, 1990.
[14] P. Hartemann, "Effective and intrinsic surface impedances of high-T_c superconducting thin films," *IEEE Trans. Appl. Superconduct.*, vol. 2, pp. 228–235, Dec. 1992.
[15] J. Wosik, R. A. Kranenburg, J. C. Wolfe, V. Selvamanickam, and K. Salama, "Millimeter wave surface resistance of grain-aligned $Y_1Ba_2Cu_3O_x$ bulk material," *J. Appl. Phys.*, vol. 69, pp. 874–879, 1991.
[16] *Microwave Engineer's Handbook*. Norwood, MA: Artech House Inc., 1984, vol. 1, pp. 180–181.
[17] A. M. Portis, *Electrodynamics of High-Temperature Superconductors*, ser. Lecture Notes in Physics. Singapore: World Sci., 1992, vol. 48.
[18] P. A. Smith, N. MacNalford, and T. W. Button, "Frequency dependence of surface resistance of bulk high temperature superconductors," *Electron. Lett.*, vol. 26, pp. 1486–1487, 1990.
[19] R. Pinto, "Microwave surface resistance of high-T_c superconducting films," in *Studies of High Temperature Superconductors*, A. V. Narlikar, Ed. New York: Nova Sci., 1996, vol. 17, pp. 147–173.
[20] D. A. Bonn, S. Kamal, K. Zhang, R. Liang, D. J. Barr, E. Klien, and W. N. Hardy, "Comparison of influence of Ni and Zn impurities on electromagnetic properties of $YBa_2Cu_3O_{6.95}$," *Phys. Rev. B, Condens. Matter*, vol. 50, pp. 4051–4063, 1994.
[21] Y. Kobayashi, T. Imai, and H. Kayano, "Microwave measurement of temperature and current dependences of surface impedance of high-T_c superconductors," *IEEE Trans. Microwave Theory Tech.*, vol. 39, pp. 1530–1538, Sept. 1991.
[22] S. Y. Lee, B. J. Soh, J. W. Ahn, J. Y. Cho, B. H. Park, C. S. Jung, V. B. Federov, A. G. Denisov, Y. H. Kim, T. S. Hahn, S. S. Choi, B. Oh, and S. H. Moon, "Use of a dielectric- loaded cylindrical cavity in measurements of the microwave surface resistance of high-T_c superconducting thin films," *IEEE Trans. Appl. Superconduct.*, vol. 7, pp. 2013–2017, June 1997.
[23] M. J. Lancaster, Z. Wu, T. S. M. Maclean, and N. MacNalford, "High temperature superconducting cavity for measurement of surface resistance," *Cryogen.*, vol. 30, pp. 1048–1050, 1990.

Mukul Misra was born in Lucknow, India, in 1969. He received the B.Sc. and M.Sc. degrees in physics from the Lucknow University, Lucknow, India, in 1990 and 1993, respectively, and the Ph.D. degree from the University of Delhi, Delhi, India, in 2000.

In early 1995, he joined the National Physical Laboratory, New Delhi, India. Since 1995, he has been investigating the various aspects effecting the accuracy of the microwave surface impedance measurement of high-temperature superconductors by resonant techniques. His current research interest includes microwave characterization of high-temperature superconducting thin films and their application for microwave passive devices.

Dr. Misra received a 1994 Research Fellowship Award presented by the Council of Scientific and Industrial Research, India.

N. D. Kataria was born in Taunggyi, Myanmar, in 1948. He received the B.Sc. (with honors), M.Sc. and Ph.D. degrees in physics from the University of Delhi, Delhi, India, in 1970, 1972, and 1977, respectively.

Since 1977, he has been a Scientist at the National Physical Laboratory, New Delhi, India. From 1980 to 1982, he visited the Physikalisch-Technische Bundesanstalt (PTB), Braunschweig, Germany, where he was involved on LTS Josephson junctions and superconducting quantum interference devices (SQUID's). From 1989 to 1991, he returned to the PTB, as a Contract Scientist under Volkswagen-Stiftung, where he was involved with the growth and device fabrication of HTS thin film. Since 1992, he has been involved with HTS thin-film processing, microwave measurement, and device application of HTS thin films. His current research interest is in the area HTS passive devices and high-Q dielectric resonators for frequency stable oscillators. He has authored many scientific papers and contributed chapters in two books on microwave characterization of HTS.

Dr. Kataria is a member of the Indian Cryogenic Council. He was the recipient of a Deutscher Academischer Austauschdienst (DAAD) Fellowship (1980–1982) and the 1990 A. N. Chatterjee Memorial Award.

G. P. Srivastava (SM'75) received the M.Sc. and D.Phil. degrees from the University of Allahabad, Allahabad, India, in 1954 and 1957, respectively.

From 1955 to 1960, he taught at the University of Allahabad and the University of Gorakhpur. In 1960, he joined the National Research Council of Canada. In 1962, he joined the University of Jodhpur, and moved to the University of Delhi, Delhi, India, in 1965, where he became a Full Professor in 1974. From 1980 to 1983, he was Head of Department of Physics and Astrophysics, and Head of the Department of Electronic Science, which was created at his initiative, from 1985 to 1988. He served the faculties of science and interdisciplinary and applied sciences as Dean from 1981 to 1983 and 1985 to 1988, respectively. He was at the University of Sheffield from 1969 to 1970, the University of Queensland from January to September 1975, and the University of Pierre and Marie Curie in 1976 for three months. He has made significant contribution in areas of microwave spectroscopy, Gunn effects, striplines, and laser-induced nonlinear optical effects. He has published over 200 papers in national and international journals and has presented approximately 70 papers at national and international conferences. His current fields of interest are superconductor electronics and microwave antenna. He was central in establishing the Asia–Pacific Microwave Conference, which is held annually in the Asia–Pacific region.

Dr. Srivastava is Fellow of the National Academy of Sciences and Institute of Electronics and Telecommunication Engineers, India.